Advanced Steel Construction – Vol. 18 No. 2 (2022) 552–560
DOI:10.18057/IJASC.2022.18.2.4

SEISMIC PERFORMANCE EVALUATION OF STEEL FRAMES WITH DAMPERS ADDED ON EXISTING STRUCTURES

Jin-Peng Tan [1], Dan-Guang Pan [1, 2, *] and Xiang-Qiu Fu [1]

[1] *Department of Civil Engineering, University of Science and Technology Beijing, Beijing 100083, China*
[2] *Beijing Key Laboratory of Urban Underground Space Engineering, School of Civil and Resource Engineering, University of Science and Technology Beijing, Beijing 100083, China*
** (Corresponding author: E-mail: pdg@ustb.edu.cn)*

ABSTRACT

The steel frames with dampers added on the top of existing structures would lead to highly non-proportional damped systems whose conventional seismic response analysis is substantially time-consuming. This paper aims to propose a real-mode-based complex mode superposition method (RMCMSM) with high computational efficiency and high accuracy. The method transforms the linear combination of complex modes into real modes with complex coefficients. It significantly reduces the time to solve complex eigenvalues and the number of complex operations, and improve computational efficiency. An ideal 2-DOFs system is used to investigate the effects of additional dampers in adding stories on modal damping ratios, coupling index and the seismic response. A real-world 5-storey structure was further analyzed to demonstrate the accuracy and efficiency of the proposed method. The numerical results show that, when the equivalent damping ratio of the additional damper increases, the stronger the non-proportionality of the system, the significantly lower the seismic response of the top layer. When designing the steel structure for the new storeys, the additional mass should be minimized and the natural frequency ratio of the overall structure should remain on the interval between 0.6 and 1.2 so that the damping effect of the additional dampers can be fully utilized. Consequently, the overall seismic performance can be enhanced.

ARTICLE HISTORY

Received: 9 June 2021
Revised: 11 September 2021
Accepted: 14 September 2021

KEYWORDS

Vertically mixed structure;
Seismic response;
Additional damper;
Non-proportional damping;
Complex mode superposition method

1. Introduction

Storey-adding with light steel frames on the top of existing structures are frequently applied in civil engineering due to their economic and functional benefits. These vertically mixed structures are usually non-proportional damping matrix systems caused by the irregularity of damping distribution over a substructure and a superstructure [1-3]. To improve the earthquake resistant performance of the superstructure, viscoelastic dampers would be added to the steel frames which further strengthen the coupling degree of the damping matrix to form the highly non-proportional damped system [4-6].

No pertinent code provisions guide the seismic analysis of such kind of structures [7,8]. Although the seismic response of a vertical mixed structure can be obtained by direct integration and frequency domain methods, the modal superposition method is considered more preferable because it is conceptually simple, effective, and convenient to apply the response spectrum to estimate the maximum response value. Therefore, most of the research work has been focused on decoupling the damping matrix of vertically mixed structures. In general, three approaches can be applied to decouple the damping matrix, namely, physical decoupling, decoupling by real mode and decoupling by complex mode.

The physical decoupling directly ignores the interaction of the two parts and considers substructure and superstructure as two independent systems. In this way, each subsystem is modelled with its own damping ratio, thus damping irregularity is avoided. The method is reasonable when the mass of the superstructure is considerably smaller than that of the substructure. Therefore, it can be used to analyze equipment-structure system [9,10]. However, it would cause significant errors when the masses of different parts are comparable [11].

In the second method, decoupling by real mode is to simplify the non-proportional damping to a proportional one. Usually, the damping ratio is assumed to be 2% for steel and 5% for concrete structures. Some engineers set uniform damping ratio equal to 2%, which will underestimate the consuming energy performance of the concrete part and lead to too conservative results. Cronin [12] forced the converted damping matrix to be diagonalized by ignoring non-diagonal terms. Huang et al. [13] also used the diagonal term to calculate the equivalent modal damping ratio. Papageorgiou and Gantes [14] proposed the damping ratio of complex modal analysis as the equivalent modal damping ratio of the real mode. Roesset et al. [15] used the energy ratio as the weighting and proposed the weighted modal damping ratio. The equivalent uniform damping ratio method and the modal strain energy (MSE) method are commonly used as approximate procedures for irregular damping conditions[16-24]. The essence of these methods can be seen as forced diagonalization. It would be very convenient for practical design and give reasonable results for systems with weakly non-proportional damping. However, for highly non-proportional damping, ignoring the effect of off-diagonal terms would cause significant errors [25-26]. In order to improve the accuracy of the results, Ibrahimbegovic and Wilson [27], Kim [28] and Aureli [29] proposed iterative solution method that consider the effects of off-diagonal terms.

In the third method, the modal superposition with complex modes has been applied to decouple the non-proportional damping matrix. Foss [30] proposed a state-space method to obtain the accurate complex modes and well established the complex modal superposition method. However, the most prominent drawback of accurate modal analysis in state space is that it requires about eight times the numerical work of calculating the undamped real mode shapes [27] and has hindered the wider application. In fact, the non-proportional damping system of vertical mixed structures can be regarded as modified from the proportional damping system, so the dynamic characteristics and responses can be determined by the perturbation method to improve the calculation efficiency. Cha [31] used the modes of an undamped system as a basis to find the first-order perturbation solution of an arbitrary but weakly non-proportional damped system. Hraˇcov [32] used the first-order perturbation method to evaluate the complex eigensolutions of a linear proportional system supplemented by a viscous damper. Recently, Pan et al [33] proposed a modal perturbation method (MPM) which can be used to analyze the eigenvalue problem of a highly non-proportionally damped system.

The aim of this paper is to propose a method with both computational efficiency and precision improved, called a real-mode-based complex mode superposition method (RMCMSM)， for seismic response analysis of light-weight steel storey-adding buildings with additional damping. After obtaining the real modes of the undamped system, this method first uses the modal perturbation method to express the complex mode as a linear combination of real modes. The complex mode superposition method is transformed into the real mode superposition method with complex coefficients to improve the calculation efficiency. On this basis, the building is simplified as a 2-DOFs system, which includes the existing and storey-adding parts idealized as 1-DOF respectively, to investigate the influence of additional dampers on the system's modal damping ratios, coupling index and the seismic response of the structure. And, compared with the traditional real-mode superposition method, the influence of off-diagonal elements of the damping matrix on the seismic response is discussed. Finally, a real-world 5-storey structure with 4 layers of existing structure plus a new layer of steel structure with dampers is used to investigate the effect of additional dampers on the seismic response and the accuracy and efficiency of the proposed method.

2. Construction of damping matrix

A typical steel frame with dampers adding on existing structure (SFDS) is shown in Fig.1. Given the stiffness matrix, mass matrix and damping matix of the subsystems of their own, then the total matrix can be expressed as:

$$[m]=[m]_a+[m]_e \tag{1}$$

$$[c]=[c]_d+[c]_a+[c]_e \tag{2}$$

$$[k]=[k]_a+[k]_e \tag{3}$$

in which [*m*], [*c*] and [*k*] are the mass matrix, damping matrix and stiffness matrix respectively; $[c]_d$ represents the contribution of the dampers to the total damping matrix; the subscripts *a* and *e* denote the subsystems of storey-adding and existing structure respectively;. the $[c]_i$ ($i=a,e$) can be obtained by Rayleigh's method [20], that is:

$$[c]_i=\alpha_i[m]_i+\beta_i[k]_i \tag{4}$$

$$\begin{Bmatrix}\alpha_i\\ \beta_i\end{Bmatrix}=\frac{2\zeta_i}{\omega_m+\omega_n}\begin{Bmatrix}\omega_m\omega_n\\ 1\end{Bmatrix} \tag{5}$$

in which ζ_a and ζ_e are the damping ratios of storey-adding and existing structure respectively; ω_m and ω_n are the two specified reference natural frequencies of the complete structure.

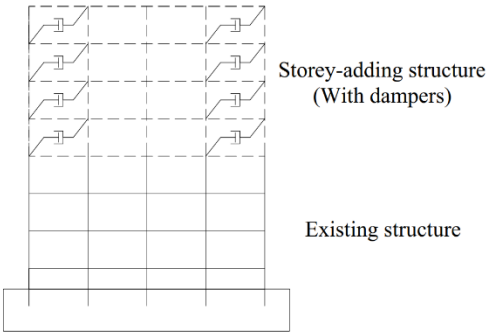

Fig. 1 A schematic model of SFDS

3. Formulation for real-mode-based complex mode superposition method

3.1. Modal perturbation method for complex eigenvalue

For the steel frames adding on the top of existing structures with *N* degrees of freedom (*N*-DOFs), the equation of motion under seismic excitation can be expressed as in the state space[30]:

$$[A]\{\dot{y}\}+[B]\{y\}=\{F\}\ddot{u}_g \tag{6}$$

$$\{y\}=\begin{Bmatrix}\{u\}\\ \{\dot{u}\}\end{Bmatrix},[A]=\begin{bmatrix}[c] & [m]\\ [m] & [0]\end{bmatrix},[B]=\begin{bmatrix}[k] & [0]\\ [0] & -[m]\end{bmatrix},\{F\}=\begin{Bmatrix}-[m]\{\iota\}\\ \{0\}\end{Bmatrix} \tag{7}$$

in which $\{u\}$, $\{\dot{u}\}$ and $\{\ddot{u}\}$ are the displacement, velocity and acceleration vectors with the dimension $N\times1$ respectively, $\{\iota\}$ is the influence vector which represents the displacements resulting from a unit support displacement, The related eigenvalue equation is:

$$(\gamma[A]+[B])\{\psi\}=\{0\} \tag{8}$$

in which γ is complex eigenvalue, and $\{\psi\}$ is their associated complex mode shapes. For a system with *N*-DOFs, there are *N* pairs of conjugate eigenvalues and associated eigenvectors. However, the seismic response would be accurately approximated by a smaller number of pairs *r* of modes in the complex modal superposition. The aim of the MPM is to obtain the first *r* eigenvalues γ_j and their associated eigenvectors $\{\psi_j\}$ (*j*=1, 2, …, *r*). Then, the conjugate eigenvalues and eigenvectors can be directly calculated by $\gamma_{j+r}=\bar{\gamma}_j$, and $\{\psi_{j+r}\}=\{\bar{\psi}_j\}$ (*j*=1, 2, …, *N*).

In the MPM [33], the corresponding equivalent proportionally damped system of the non-proportional damped system is defined by [*m*], [*k*] and a uncoupled modal damping ratio ζ_j, which is estimated by the modal strain energy method (MSEM) [34], that is,

$$\zeta_j=\frac{\{\phi_j\}^T[c]\{\phi_j\}}{2M_j\omega_j} \tag{9}$$

in which the ω_j and $\{\phi_j\}$ (*j*=1, 2, …, *n*) are the j^{th} undamped circular natural frequencies and its associated modes; $M_j=\{\phi_j\}^T[m]\{\phi_j\}$ is the modal mass. Then, the complex eigenvalues and their associated complex mode shapes of the equivalent proportionally damped system can be expressed as:

$$s_j=-\zeta_j\omega_j+i\omega_j\sqrt{1-\zeta_j^2},\{\eta_j\}=\begin{Bmatrix}\{\phi_j\}\\ s_j\{\phi_j\}\end{Bmatrix}\ (j=1,2,\ldots,n) \tag{10}$$

For *j*>*n*, $s_j=\bar{s}_{j-n}$, $\{\eta_j\}=\{\bar{\eta}_{j-n}\}$. $i=\sqrt{-1}$ is the unit complex.

The j^{th} complex eigenvalue and its associated mode of Eq. (8) are related to those of the corresponding proportionally damped system in following ways:

$$\gamma_j=s_j+\Delta s_j \tag{11}$$

$$\{\Psi_j\}=\begin{Bmatrix}\{\varphi_j\}\\ \gamma_j\{\varphi_j\}\end{Bmatrix}=\{\eta_j\}+\sum_{k=1,k\neq j}^{2n}\{\eta_k\}q_{kj}=[\eta]\{q_j\} \tag{12}$$

$$[\eta]=\begin{bmatrix}[\phi] & [\phi]\\ [\phi]\langle s\rangle & [\phi]\langle\bar{s}\rangle\end{bmatrix} \tag{13}$$

in which Δs_j is the eigenvalue perturbation; $\{\varphi_j\}$ is the complex modes; q_j is a complex coefficient; $\langle*\rangle$ denotes the * is a diagonal matrix; $[\phi]$ is a *N*×*n* mode matrix composed of the first *n* real modes $\{\phi_j\}$. Defining:

$$x_k=\begin{cases}\Delta s_j/s_j & k=j\\ q_{kj} & k\neq j\end{cases} \tag{14}$$

In MPM, the $\{x\}$ can be obtained by solving the algebraic equation:

$$\left(\begin{bmatrix}[D_{11}] & [D_{12}]\\ [D_{21}] & [D_{22}]\end{bmatrix}+x_j\begin{bmatrix}[E_{11}] & [E_{12}]\\ [E_{21}] & [E_{22}]\end{bmatrix}\right)\{x\}=\begin{Bmatrix}\{R_1\}\\ \{R_2\}\end{Bmatrix} \tag{15}$$

where $[D_{11}]$, $[D_{12}]$, $[D_{21}]$, $[D_{22}]$, $[E_{11}]$, $[E_{12}]$, $[E_{21}]$ and $[E_{22}]$ are all *n*×*n* square matrices; $\{R_1\}$ and $\{R_2\}$ are *n*×1 vectors; $\{x\}$ are 2*n*×1 vectors. The above *n*×*n* square matrices can be expressed as:

$$[D_{11}]=[C]+2\langle M\rangle\langle s\rangle+\frac{1}{s_j}\langle M\rangle_{j=0}\langle\omega^2-s^2\rangle \tag{16}$$

$$[D_{12}]=[D_{21}]=[C]+\langle M\rangle\langle s+\bar{s}\rangle \tag{17}$$

$$[D_{22}]=[C]+2\langle M\rangle\langle\bar{s}\rangle+\frac{1}{s_j}\langle M\rangle\langle\omega^2-s^2\rangle \tag{18}$$

$$[E_{11}]=[C]_{j=0}+2\langle M\rangle_{j=0}\langle s\rangle \tag{19}$$

$$[E_{12}]=[C]+\langle M\rangle\langle s+\bar{s}\rangle \tag{20}$$

$$[E_{21}]=[C]_{j=0}+2\langle M\rangle_{j=0}\langle s+\bar{s}\rangle \tag{21}$$

$$[E_{22}]=[C]+2\langle M\rangle\langle\bar{s}\rangle \tag{22}$$

in which $[C]=[\phi]^T[c][\phi]$; $\langle M\rangle=[\phi]^T[m][\phi]$; $[C]_{j=0}$ and $\langle M\rangle_{j=0}$ denote that the j^{th} column of $[C]$ and $\langle M\rangle$ are zero. The $n\times1$ vectors are given below:

$$\{R_1\}=-\left\{C_{1j}\quad \mathrm{L}\quad C_{(j-1)j}\quad C_{jj}+2s_jM_j+\frac{\omega_j^2-s_j^2}{s_j}M_j\quad C_{(j+1)j}\quad \mathrm{L}\quad C_{nj}\right\}^T \tag{23}$$

$$\{R_2\}=-\left\{C_{1j}\quad \mathrm{L}\quad C_{(j-1)j}\quad C_{jj}+(\bar{s}_j+s_j)M_j\quad C_{(j+1)j}\quad \mathrm{L}\quad C_{nj}\right\}^T \tag{24}$$

Once $\{x\}$ is determined by Eq. (15), the j^{th} eigenvalue and its associated complex mode of vibration of the non-classically damped system can be obtained by Eqs. (11) and (12). Then, the j^{th} pseudo undamped natural frequency $\bar{\omega}_j$ and damping ratio $\bar{\zeta}_j$ can be expressed as:

$$\bar{\omega}_j=|\gamma_j|,\bar{\zeta}_j=-\mathrm{Re}(\gamma_j)/|\gamma_j| \tag{25}$$

$\{q_j\}$ can be expressed as:

$$\{q_j\}=\begin{Bmatrix}q_{uj}\\ q_{lj}\end{Bmatrix} \tag{26}$$

in which $\{q_{uj}\}$ and $\{q_{lj}\}$ are the upper and lower n elements respectively. Then, the j^{th} complex mode $\{\varphi_j\}$ can be expressed as the linear combination of real modes, that is:

$$\{\varphi_j\}=[\phi]\{\hat{q}_j\} \tag{27}$$

$$\{\hat{q}_j\}=\{q_{uj}\}+\{q_{lj}\} \tag{28}$$

Taking j from 1 to r in turn, the complex mode matrix $[\varphi]$ can be expressed as:

$$[\varphi]=[\phi][\hat{q}] \tag{29}$$

in which $[\varphi]$ is a $N\times r$ matrix.

3.2. Real-mode-based complex mode superposition method on seismic response

By complex mode superposition, the state vector $\{y\}$ in state equation (6) can be expanded in terms of complex eigenvectors $\{\psi_j\}$, that is:

$$\{y\}=\begin{Bmatrix}\{u\}\\ \{\dot{u}\}\end{Bmatrix}=2\,\mathrm{Re}\left(\sum_{j=1}^{r}\{\psi_j\}z_j\right) \tag{30}$$

Then, the uncoupled equation for the j^{th} (j=1, 2, …, r) complex mode of vibration is:

$$\dot{z}_j-\gamma_jz_j=\Gamma_j\ddot{u}_g(t) \tag{31}$$

$$\Gamma_j=-\{\varphi_j\}^{\mathrm{T}}[m]\{\iota\}/a_j \tag{32}$$

where $a_j=\{\Psi_j\}^{\mathrm{T}}[A]\{\Psi_j\}$. By using Eqs. (27) and (12), Γ_j and a_j can be expressed as:

$$\Gamma_j=-\{\hat{q}_j\}^T[\phi]^T[m]\{\iota\}/a_j \tag{33}$$

$$a_j=\{q_j\}^T[\eta]^T[A][\eta]\{q_j\} \tag{34}$$

By substituting Eq. (13) into Eq. (34), a_j can be rewritten as:

$$a_j=\{\hat{q}_j\}^T[C]\{\hat{q}_j\}+2\sum_{i=1}^{n}\left(s_i\hat{q}_{uij}+\bar{s}_i\hat{q}_{lij}\right)M_i\hat{q}_{ij} \tag{35}$$

The solution of Eq. (31) can be solved by Duhamel's integration [35,36] or frequency domain method [37,38], and a numerical procedure based on Duhamel's integration was adopted in this paper. Once z_j is determined, the displacement can be expressed as:

$$\{u\}=2\,\mathrm{Re}\left([\phi][\hat{q}]\{z\}\right) \tag{36}$$

It can be seen from Eqs. (33), (35) and (36) that the real-mode-based complex mode superposition method (RMCMSM) reduces the number of times of complex multiplication. For example, a_j which needs $2N\times2N$ times of complex multiplication in the state-space method, needs only $n\times n+n$ times in the proposed method. In addition, the displacement of each step in Eq. (36) of complex multiplication numbers is reduced from $N\times r$ to $n\times r$. Usually, n is far less than N so the RMCMSM will improve the calculation efficiency significantly.

3.3. The algorithm workflow

In order to make the procedure of the algorithm clearer, the workflow of the proposed method is shown in Fig. 2.

The algorithm is executed in five steps:

Step 1: Construction of mass matrix $[m]$, damping matrix $[c]$ and stiffness matrix $[k]$ from Eq. (1), Eq. (2)and Eq. (3).

Step 2: Calculate the first n undamped circular natural frequencies ω_j and its associated real modes $\{\phi_j\}$. Then, calculate the modal damping matrix $[C]$, and obtain the modal damping ratio ζ_j, the complex eigenvalues s_j and their associated complex mode shapes $\{\eta_j\}$ of the equivalent proportionally damped system by Eq. (9) and Eq. (10), and set j=1.

Step 3: Form the $[D_{ij}]$, $[E_{ij}]$, and $[R_i]$ (i, j=1,2), then obtain $\{x\}$ by Eq. (15),

Step 4: Based on $\{x\}$, obtain the γ_j by Eq. (11) and $\{\hat{q}_j\}$ by Eq. (28). Then, set j=j+1, and go back to Step 3 until j=r which r is the desirable highest mode.

Step 5: Obtain a_j, Γ_j by Eq. (35) and Eq. (33), then taking j from 1 to r in turn can solve $\{z_j\}$ from Eq. (31).

Step 6: In the end, the displacement $\{u\}$ can be calculated by Eq. (36).

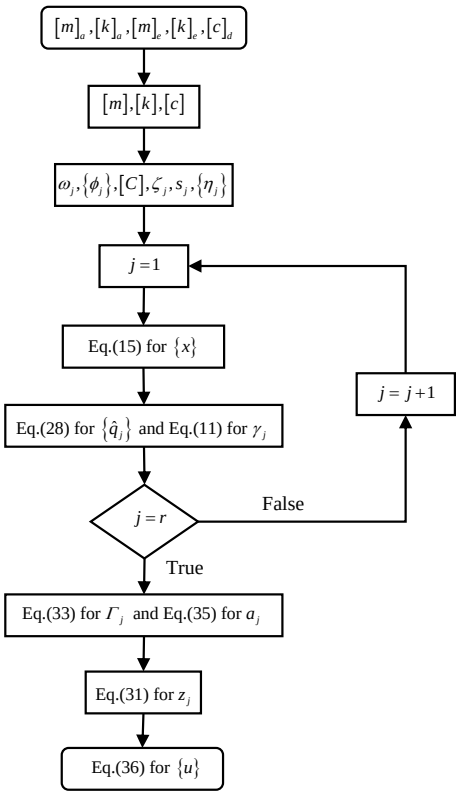

Fig. 2 Flowchart of the proposed method

4. Parametric study

An ideal MDOF storey-adding structure with dampers as shown in Fig.1 can be approximately simplified as an equivalent 2-DOFs system in Fig.3, following Huang[20] and Papageorgiou Gantes[14]. Firstly, two submatrices $[k]_i$ and $[m]_i$, where $i = a, e$, each representing the contribution of the corresponding part of the structure to the total structure matrix, can be expressed as:

$$[m]_e=\begin{bmatrix} m_e & \\ & 0 \end{bmatrix},[m]_a=\begin{bmatrix} 0 & \\ & m_a \end{bmatrix} \tag{37}$$

$$[k]_e=\begin{bmatrix} k_e & 0 \\ 0 & 0 \end{bmatrix},[k]_a=\begin{bmatrix} k_a & -k_a \\ -k_a & k_a \end{bmatrix} \tag{38}$$

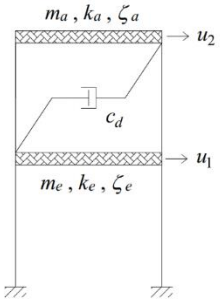

Fig. 3 Equivalent 2-DOFs structure

The damping ratios of two subsytems are defined as $\zeta_a = 0.02$ and $\zeta_e = 0.05$. A damper in the upper structure denotes additional energy consumption. The parameters of the dampers are expressed as:

$$c_d = 2\zeta_d \omega_a m_a \tag{39}$$

$$[c]_d=\begin{bmatrix} c_d & -c_d \\ -c_d & c_d \end{bmatrix} \tag{40}$$

in which ζ_d is the equivalent damping ratio of the damper. In order to investigate the effect of the dampers and the properties of the two subsystems, three parameters are defined:

$$R_m=\frac{m_a}{m_e}, R_\omega=\frac{\omega_a}{\omega_e}, R_\zeta=\frac{\zeta_a+\zeta_d}{\zeta_e} \tag{41}$$

Without loss of generality, the mechanical parameters of the system are chosen as m_e=4×10^{6}kg, k_e=1×10^{6}kN/m. Then, the other parameters can be derived as:

$$m_a = R_m m_e, k_a = R_\omega{}^2 k_e R_m, c_d = 2(R_\zeta \zeta_e - \zeta_a)\sqrt{k_a m_a} \tag{42}$$

For non-proportionally damped systems, the modal damping matrix $[C]$ is not diagonal. The coupling index α can be expressed as [39]:

$$\alpha=\max\left(\frac{C_{lk}^2}{C_{ll}C_{kk}}\right) \quad (l \neq k) \tag{43}$$

which represents the degree of non-proportional damping.

4.1. Influences of dampers on modal damping ratios

Normally, the mass of the added layer structure is less than the mass of the main structure, without loss of generality. The following mainly analyzes the change law of the modal damping ratio of the system when R_m is equal to 1/8, 1/4 and 1/2 respectively. Table 1 lists the undamped natural frequencies of various R_m when $R_\omega = \sqrt{2}/2$.

Table 1
The undamped natural frequencies (Hz) of the 2-DOFs system

No. of modes	R_m		
	1/8	1/4	1/2
1	1.687	1.617	1.510
2	2.657	2.773	2.968

The modal damping ratios which are calculated by MPM and MSEM over the (R_ω - R_ζ) plane are shown in Fig. 4, Fig. 5 and Fig. 6. In addition, the coupling index α is also depicted to illustrate the degree of non-proportional damping. R_ζ=0.4 represents that there is no damper in the system. In the MPM, all the 4 modes $\{\eta_j\}$ of the 2-DOFs system are used in Eq. (12) to obtain the exact complex eigenvector $\{\psi_j\}$ by MPM [33]. It can be seen that: 1) When $0.6 < R_\omega < 1.2$, the damper would significantly affect the modal damping ratios and the coupling index. It means that the damper would be sensitive to the damping characteristics of the system when the natural frequency of the superstructure and substructure is close. 2) Once $R_\omega > 1.5$, ζ_1 is close to 0.05 and ζ_2 is close to $0.05R_\zeta$, and when $R_\omega < 0.4$, ζ_1 is close to $0.05R_\zeta$ and ζ_2 is close to 0.05. It represents that when the natural frequency difference between the two subsystems is large, ζ_1 is determined by the lower natural frequency subsystem while the ζ_2 is determined by the higher one. 4) When R_ζ is larger than 1, coupling index α increases with the increase of additional damping. 5) The influence of mass ratio R_m on the damping ratios and coupling index is not significant. 6) The damper would cause a bigger coupling index α. With increasing ζ_d, both modal damping ratios increase, and those obtained by MSEM shows more obvious errors.

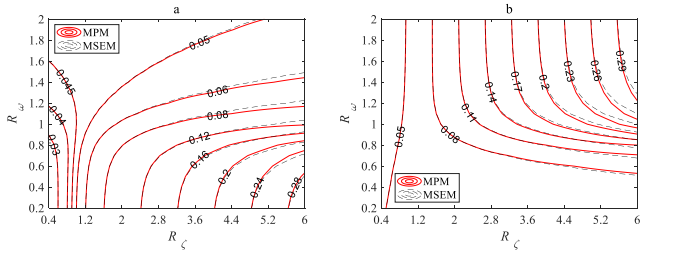

(a)modal damping ratio of the first mode ζ_1 (b)modal damping ratio of the second mode ζ_2

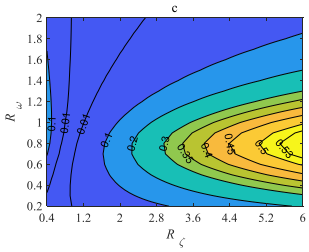

(c) coupling index α

Fig. 4 Modal damping ratios and coupling index of the 2-DOFs structure (R_m=1/8)

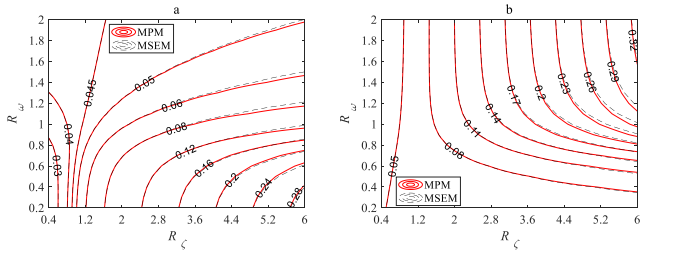

(a)modal damping ratio of the first mode ζ_1 (b)modal damping ratio of the second mode ζ_2

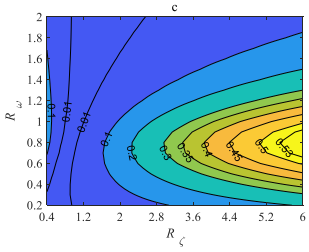

(c) coupling index α

Fig. 5 Modal damping ratios and coupling index of the 2-DOFs structure (R_m =1/4)

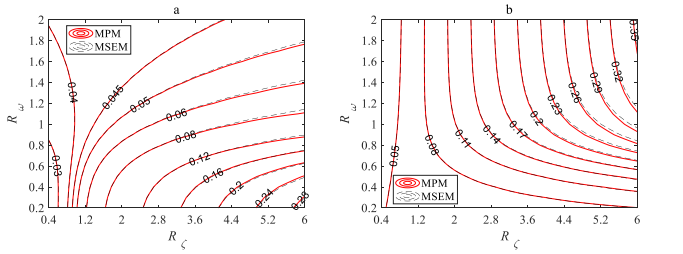

(a)modal damping ratio of the first mode ζ_1 (b)modal damping ratio of the second mode ζ_2

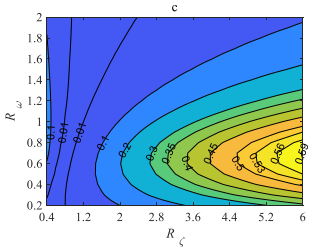

(c) coupling index α

Fig. 6 Modal damping ratios and coupling index of the 2-DOFs structure (R_m =1/2)

4.2. Influences of dampers on seismic response

The El Centro wave and Qianan wave which are classified to II site and I site respectively, with different main frequencies, are selected to investigate the influence of dampers on seismic response. The El Centro wave recorded in the California earthquake in May 1940 in the N-S direction, whose time history and Fourier spectrum are shown in Figure 7(a) and (b), consistency. The Qianan wave and its Fourier spectrum of the aftershock of the Tangshan earthquake in 1976 are shown in Fig. 7(c) and (d) , consistency. In addition, the smoothing of FFT is also shown to obtain predominant frequency. It can be seen that the predominant frequencies are 1.7 Hz of El Centro wave and 4.8Hz of Qianan wave.

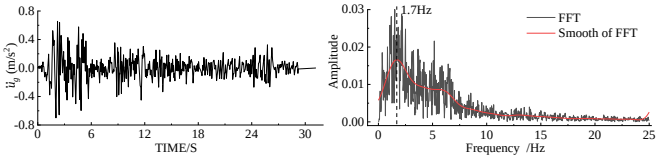

(a) acceleration time history of El Centro wave (b) Fourier spectrum of El Centro wave

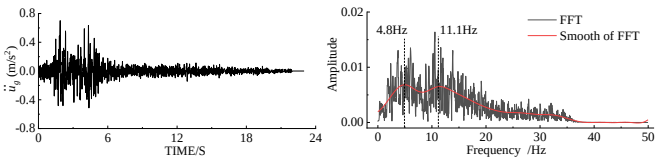

(c) acceleration time history of Qianan wave (d) Fourier spectrum of Qianan wave

Fig. 7 The acceleration time history and corresponding Fourier spectrum of input wave

The displacement amplitudes are calculated by RMCMSM, as shown in Fig. 8 and Fig. 9. Since the frequencies and modes obtained by MPM are accurate, the calculation results of RMCMSM using all modes are also accurate. When $0.6 < R_\omega < 1.2$, $R_\zeta < 5.0$, with the increase of R_ζ, the u_2 contour is a dense vertical line, which indicates that in this parameter range, the damper has an obvious seismic mitigation on the top layer. On the contrary, the contour of u_1 is nearly horizontal, which indicates that u_1 is mainly affected by R_ω, while the effect of additional damping is not significant. The increase of R_m will increase the inertial force of the system, which will cause both the reactions of u_1 and u_2 to increase. Therefore, when designing the storey-adding steel structure, the mass of the additional layer should be minimized.

When $R_\omega < 0.4$, a slight decrease of R_ω will cause a sharp increase in u_2. Moreover, the increasing of the additional damping will not cause an obvious effect on the decreasing of u_2. This shows that if the stiffness of the added-story structure is too low, it will make the displacement of the superstructure too large to control. This situation should be avoided in the design. When $R_\omega > 1.5$, it is essential to increase the cross-sectional size of the structural elements for seismic design, which will increase the cost of the structure. When $0.6 < R_\omega < 1.2$, the damping effect of the damper can be fully exerted and the structure will have both good seismic performance and economy.

At the same time, the frequency content of the input seismic wave would affect the seismic mitigation effect of the damper. Compared with the Qianan wave, the damper under the El Centro wave can reduce u_2 in a wider range of R_ω. The prominent frequency of the El Centro wave is close to the first-order natural frequency of the system. The prominent frequency of Qianan wave is close to second-order. Since the response of the structure is mainly controlled by the first mode, the damper has a better seismic mitigation effect on the El Centro wave.

If the conventional real mode superposition method (RMSM) is used to analyze the seismic response of the structure ignoring the off-diagonal terms of the damping matrix and using MSEM damping ratios, there will be certain errors. The relative error e can be expressed into:

$$e_r = \left| \frac{r - r^*}{r^*} \right| \times 100\% \tag{44}$$

in which r and r^* are the approximate and exact solution.

Fig. 10 and Fig. 11 show that the relative errors of displacements which are calculated by RMSM. Comparing with Fig. 4, Fig. 5 and Fig. 6, it can be seen that the relative errors of displacements would increase when the value of the coupling index α increases. Furthermore, the errors are obviously influenced by different types of seismic waves. When α>0.2, the relative errors by RMSM would be more than 10%.

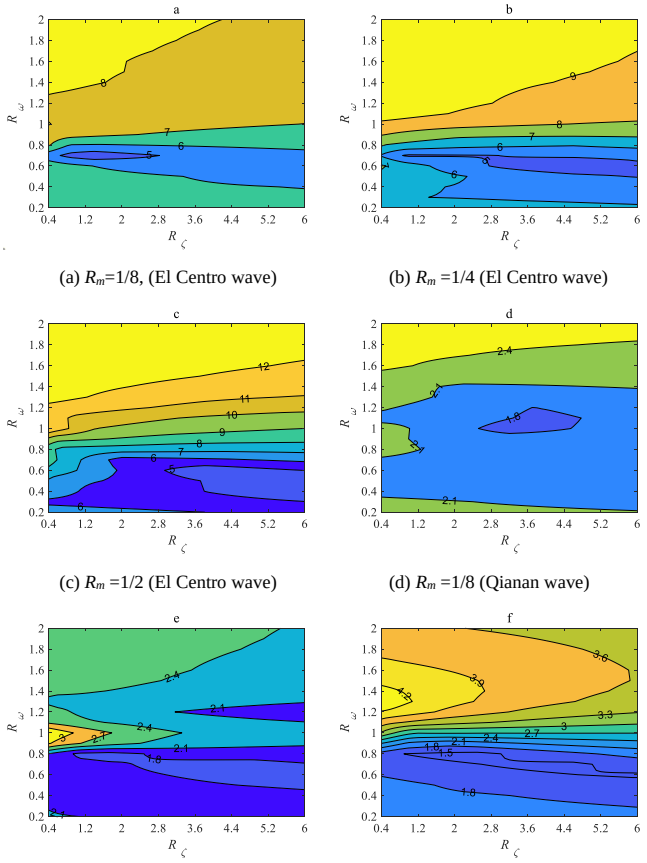

(a) R_m=1/8, (El Centro wave) (b) R_m =1/4 (El Centro wave)

(c) R_m =1/2 (El Centro wave) (d) R_m =1/8 (Qianan wave)

(e) R_m =1/4 (Qianan wave) (f) R_m =1/2 (Qianan wave)

Fig. 8 The displacement amplitudes of u_1 (mm)

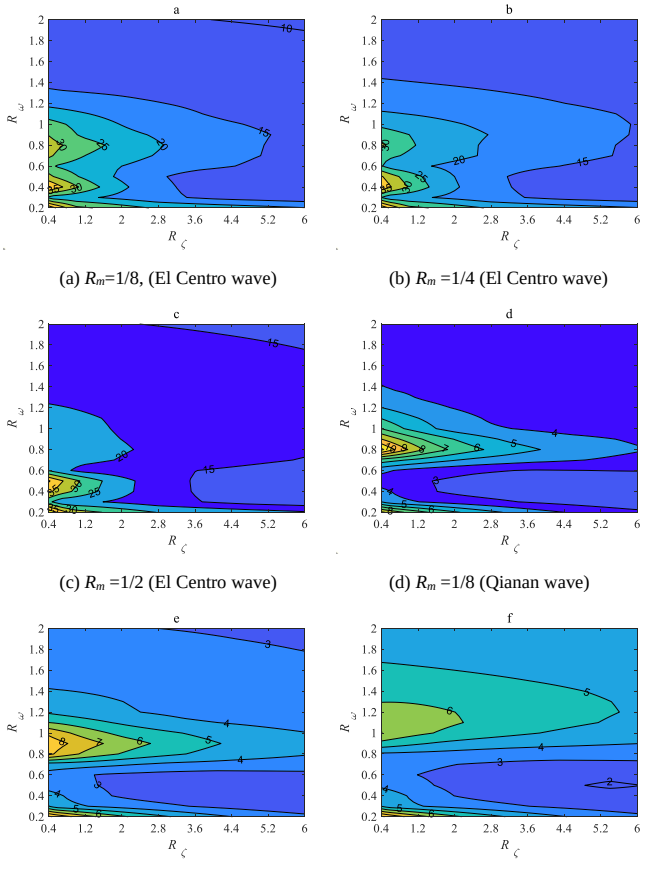

(a) R_m=1/8, (El Centro wave) (b) R_m =1/4 (El Centro wave)

(c) R_m =1/2 (El Centro wave) (d) R_m =1/8 (Qianan wave)

(e) R_m =1/4 (Qianan wave) (f) R_m =1/2 (Qianan wave)

Fig. 9 The displacement amplitudes of u_2 (mm)

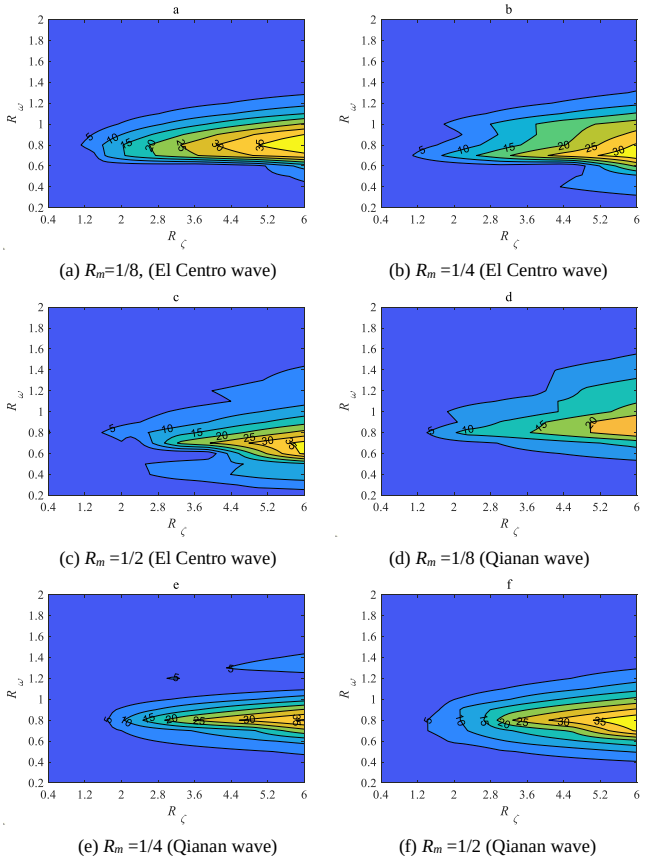

(a) R_m=1/8, (El Centro wave) (b) R_m =1/4 (El Centro wave)

(c) R_m =1/2 (El Centro wave) (d) R_m =1/8 (Qianan wave)

(e) R_m =1/4 (Qianan wave) (f) R_m =1/2 (Qianan wave)

Fig. 10 The relative errors of displacement u_1 (%)

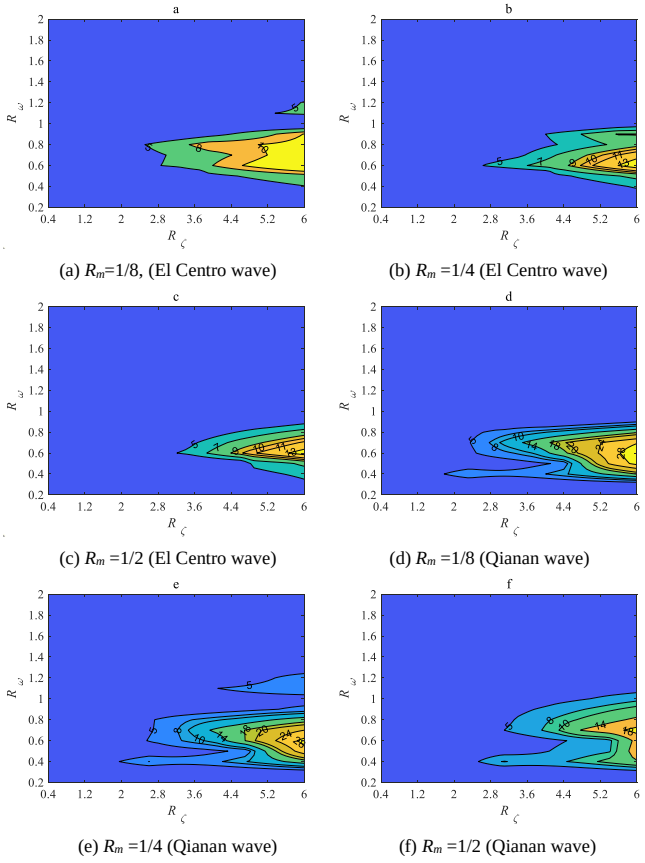

(a) R_m=1/8, (El Centro wave) (b) R_m =1/4 (El Centro wave)

(c) R_m =1/2 (El Centro wave) (d) R_m =1/8 (Qianan wave)

(e) R_m =1/4 (Qianan wave) (f) R_m =1/2 (Qianan wave)

Fig. 11 The relative errors of displacement u_2 (%)

5. Practical applications of the proposed method

A 2-DOFs structure is used to illustrate the proposed method and discuss the effect of additional damping on the seismic response of the structure. The

time consumed for the real-mode-based complex superposition and direct complex superposition will not make a significant difference. To fully explore the potential of the proposed method in engineering practices, an office building of a 4-storey concrete frame structure with an additional 6m high steel structure on top, as shown in Fig 12, is studied. The material of the existing structure is C30 concrete, whose material parameters are: density ρ_c=2500kg/m^3, modulus of elasticity E_c=3×10^{10} Pa and damping ratio ζ_c=0.05. In addition to the self-weight of the frame structure, the applied load is 10.5 kN/m for each concrete beam element. The material of the new steel structure is Q345, whose material parameters are: ρ_s=7800kg/m^3, E_s=2×10^{11} Pa and ζ_s=0.02. The applied load is 9.5kN/m for each steel beam element. In this instance, the mass ratio of the upper steel structure and the lower concrete structure $R_m = 0.164$.

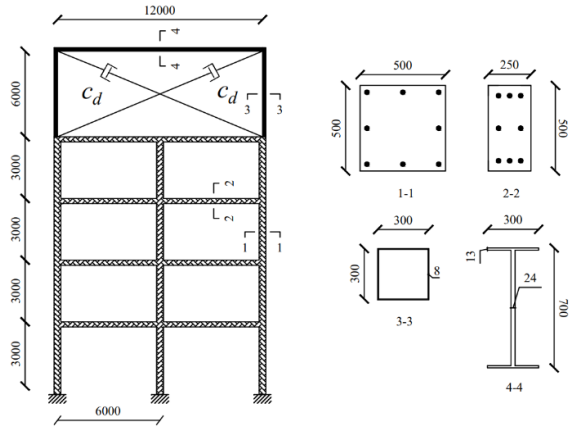

Fig. 12 An office building with mixed steel-concrete structure (unit: mm)

In order to improve the earthquake resistant performance of the storey-adding structure, the designed columns of the superstructure are 300×300×8mm square steel pipe. The frequency ratio R_ω of the upper steel structure and the lower concrete structure is 0.8. There are two dampers applied to the steel structure with damping constant c_d equal to 3.6×10^{4}N.s/m and therefore $R_\varsigma = 4$.

The finite element model of the frame structure contains 28 DOFs. The additional loads are transformed into equivalent additional masses to represent the inertial force.

Table 2 lists the accumulated mass participating factor a_m along the horizontal direction. Obviously, a_m of the first 10 modes exceed 90% and therefore 10 pairs of complex modes are used in RMCMSM and 10 real modes are used in RMSM. To calculate the Rayleigh coefficients by Eq. (5), the 1st and 10th natural frequencies of the complete structure are used as the the two specfied reference frequencies. Then, the damping matrix of the system is constructed by Eq. (2). The coupling index α of the structure is 0.51 for the structure with additional dampers (ADS). The storey-adding steel frame without dampers (NDS), whose coupling index α equals 0.15, are comparatively investigated.

Table 2
Accumulated of mass participating factor a_m (%)

Modes	1	2	3	4	5
a_m	24.93	42.23	47.18	49.28	66.95
Modes	6	7	8	9	10
a_m	66.95	67.66	85.02	85.02	95.62

5.1. MPM for eigenvalue problem

For practical engineering, the incomplete set of undamped modes, which includes 8 additional modes [40], will be used in Eq. (12). According to the results listed in Table 2, the first 10 pairs of complex eigenvalues of the non-proportional damped system are used in the mode superposition to calculate the seismic response. Then, the first 18 undamped modes are used in MPM. Table 3 lists the first 10 pseudo undamped natural frequencies and damping ratios by MPM with n=18 for the structure with and without additional dampers. For comparison, the results obtained by the MSEM and exact solution and are also listed. The relative errors of natural frequencies and damping ratios are shown in Table 4. It can be seen that the errors of natural frequencies and damping ratios obtained by the MPM are always less than 0.015%. The relative errors of those obtained by the MSEM would be less than 1.267%.

Table 3
The natural frequencies (Hz) and damping ratios of the frame system

Mode	ADS						NDS					
	Natural frequencies			Damping ratios			Natural frequencies			Damping ratios		
	Exact	MPM	MSEM	Exact	MPM	MSEM	Exact	MPM	MSEM	Exact	MPM	MSEM
1	1.690	1.690	1.669	0.112	0.112	0.113	1.669	1.669	1.669	0.026	0.026	0.026
2	3.084	3.084	3.117	0.139	0.139	0.138	3.117	3.117	3.117	0.025	0.025	0.025
3	8.957	8.957	8.972	0.038	0.038	0.038	8.972	8.972	8.972	0.023	0.023	0.023
4	17.581	17.580	17.584	0.036	0.036	0.036	17.584	17.584	17.584	0.033	0.033	0.033
5	21.884	21.883	21.877	0.025	0.025	0.025	21.884	21.883	21.877	0.025	0.025	0.025
6	21.915	21.915	21.908	0.025	0.025	0.025	21.915	21.915	21.908	0.025	0.025	0.025
7	26.746	26.746	26.746	0.047	0.047	0.047	26.746	26.746	26.746	0.047	0.047	0.047
8	28.403	28.403	28.404	0.050	0.050	0.050	28.403	28.403	28.404	0.050	0.050	0.050
9	43.764	43.761	43.774	0.059	0.059	0.059	43.764	43.761	43.774	0.059	0.059	0.059
10	43.784	43.781	43.794	0.059	0.059	0.059	43.784	43.781	43.794	0.059	0.059	0.059

Table 4
The relative errors (%) of natural frequencies and damping ratios of the frame system

Mode	ADS				NDS			
	Natural frequencies		Damping ratios		Natural frequencies		Damping ratios	
	MPM	MSEM	MPM	MSEM	MPM	MSEM	MPM	MSEM
1	0.001	1.267	0.002	0.166	0.000	0.015	0.000	0.006
2	0.002	1.093	0.005	1.086	0.000	0.014	0.000	0.003
3	0.001	0.163	0.005	0.359	0.000	0.000	0.000	0.000
4	0.000	0.019	0.001	0.023	0.000	0.000	0.000	0.000
5	0.003	0.032	0.000	0.043	0.003	0.032	0.000	0.043
6	0.003	0.032	0.000	0.043	0.003	0.032	0.000	0.043
7	0.000	0.001	0.000	0.000	0.000	0.000	0.000	0.000
8	0.000	0.000	0.000	0.000	0.000	0.000	0.000	0.000
9	0.007	0.022	0.015	0.017	0.007	0.022	0.015	0.017
10	0.007	0.022	0.015	0.017	0.007	0.022	0.015	0.017

5.2. Discussion on results of seismic response

The maximum horizontal displacements $u_{i\max}$, and inter-story drift angles $\theta_{i\max}=\left|u_i-u_{i-1}\right|_{\max}/h_i$ of the five floors under the El Centro and Qianan wave excitations, are respectively shown in Fig. 13 and Fig. 14. The h_i is the height of the i^{th} storey. Based on the previous results, 10 pairs of complex modes were included in the solution of Eq. (30) by the RMCMSM. The 10 undamped modes were used by the RMSM. The exact solution is the result of the complex mode superposition obtained by the state-space method based on complete complex modes.

The effect of dampers on the seismic response can be shown from Figs. 13 and 14. The displacement amplitudes of the top layer decreased from 29.85mm to 20.41mm and from 6.21mm to 4.78mm under El Centro and Qianan excitations respectively; the inter-story drift angles decreased from 1/239 to 1/395 and from 1/1000 to 1/1408 under El Centro and Qianan excitations respectively.

From the viewpoint of accuracy, the maximum horizontal displacements and inter-story drift angles obtained by RMCMSM almost coincided with those by exact solution. However, the discrepancies between the results of RMSM and those of exact solution are obvious, whether the dampers are applied or not. The relative errors of peak response are shown in Table 5 and Table 6. The errors of the RMCMSM are all less than 1.261%. However, the errors of the RMSM would reach 25.850% for the system with dampers and 12.450% for the system without dampers, which shows that the RMSM may cause significant errors for vertically mixed structures whether dampers are applied or not.

As can be seen from Table 4, despite the fact that the errors of natural frequencies and damping ratios are tiny, the RMSM would nonetheless cause significant errors due to ignoring the effect of the imaginary part of complex modes of the non-proportional damping. It means that the calculation accuracy of the RMCMSM is significantly higher than that of the RMSM.

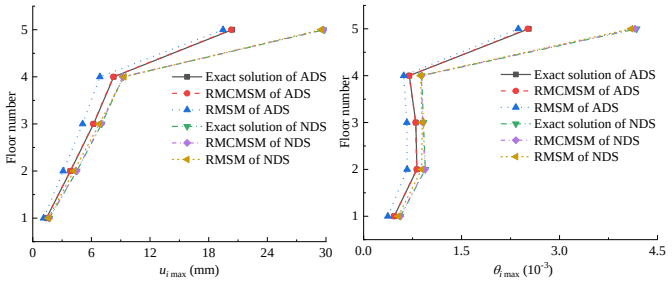

(a) Maximum lateral displacements $u_{i\max}$ (b) Maximum inter-story drift angles $\theta_{i\max}$

Fig. 13 Seismic responses of the office building under El Centro wave

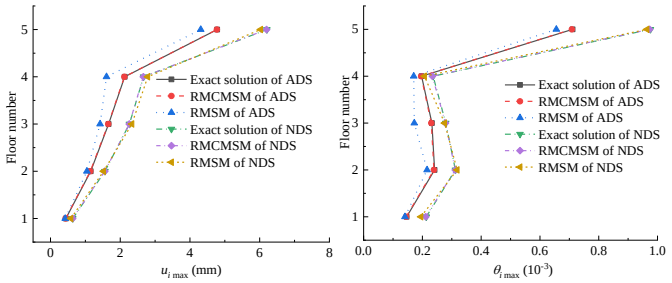

(a) Maximum lateral displacements $u_{i\max}$ (b) Maximum inter-story drift angles $\theta_{i\max}$

Fig. 14 Seismic responses of the office building under Qianan wave

Table 5
The relative errors (%) of maximum horizontal displacements and inter-story drift angles of ADS

Layers	RMCMSM				RMSM			
	El Centro		Qianan		El Centro		Qianan	
	e_u	e_θ	e_u	e_θ	e_u	e_θ	e_u	e_θ
1	0.290	0.290	1.109	1.106	20.597	20.598	3.964	3.961
2	0.429	0.623	0.888	0.952	19.096	18.400	9.384	10.574
3	0.573	0.507	0.590	0.874	18.102	17.200	14.651	25.850
4	0.552	0.507	0.402	0.674	17.120	12.243	24.526	13.555
5	0.510	0.652	0.175	0.346	4.582	6.349	9.850	7.769

Table 6
The relative errors (%) of maximum horizontal displacements and inter-story drift angles of NDS

Layers	RMCMSM				RMSM			
	El Centro		Qianan		El Centro		Qianan	
	e_u	e_θ	e_u	e_θ	e_u	e_θ	e_u	e_θ
1	0.956	0.955	0.938	0.938	6.393	6.393	8.600	8.599
2	0.729	0.651	0.435	0.163	6.685	6.165	2.670	1.921
3	0.717	1.261	0.129	0.426	3.440	1.882	3.172	1.378
4	0.547	0.461	0.335	1.079	1.082	1.951	4.407	12.450
5	0.359	0.622	0.141	0.282	1.163	2.105	2.891	1.204

5.3. Computational efficiency of RMCMSM

The RMCMSM uses the MPM to solve the characteristic equation, which is more efficient than the state-space method. Meanwhile, the complex modes of the proposed method are linearly combined with real modes, which improves the calculation efficiency due to the reduction of complex calculations and dimensions of the matrices. Table 7 compares the computation time of the RMCMSM and the state-space method with 10 pairs of complex modes for the 5-storey vertically mixed structure under excitation of El Centro wave. In Table 7, T_1 denotes the time to solve the characteristic equation, T_2 denotes the time to solve parameters Γ_j and a_j, T_3 denotes the time to solve z_j in Eq. (31), T_4 denotes the time to solve Eq. (30) in the state-space method and Eq. (36) in RMCMSM and T_a is the total calculation time.

It can be seen that the time consumed by MPM to solve the characteristic equation is less than the time for the state-space method to solve the complex characteristic equation directly. The computational efficiency of the proposed RMCMSM is also higher than that of the state-space method for the calculation of parameters Γ_j and a_j. Two methods consume the same amount of time to solve z_j in Eq. (31) for the same calculation process. However, T_1 and T_2 will increase dramatically when the number of degrees of freedom N increases, which will significantly amplify the advantages of the proposed method. Therefore, the RMCMSM outperforms the state-space method when considering both the efficiency and accuracy for the vertically mixed structures with additional dampers.

Table 7
Calculation time (ms)

Methods	T_1	T_2	T_3	T_4	T_a
State-space method	1.72	0.08	1.83	0.04	3.67
RMCMSM	1.12	0.03	1.83	0.03	3.01

6. Conclusions

Light steel frames added on existing structures are typical vertically mixed structures. For improving the seismic resistant performance, dampers are used in the steel frame which make the damping more highly non-proportional. In this paper, a real-mode-based complex mode superposition method with high accuracy and high efficiency is proposed to analyze the seismic response of non-proportional damped structures. Based on extensive analyses and numerical results, the following conclusions can be drawn:

1)The seismic responses obtained by the proposed RMCMSM almost coincided with those by exact solution. The RMCMSM reduces the calculation time of complex eigenproblem and the number of times of complex multiplication so that its time consumed is less than that of the state-space method. In general, the proposed method takes into account the calculation efficiency and accuracy and is suitable for seismic response analysis of vertically mixed structures with dampers. However, the RMSM ignore the effects of off-diagonal terms of the damping matrix and the effect of the imaginary part of complex modes to cause also the errors.

2) In general, the mass of the added layer of structure is less than that of the main structure, when $R_\omega < 0.4$ or $R_\omega > 1.5$, ζ_1 is determined by the lower natural frequency subsystem and ζ_2 is determined by the higher counterpart. When $0.6 < R_\omega < 1.2$, the system shows obvious coupling effect that the damper would significantly affect the modal damping ratios and the coupling index. In addition, a higher R_ζ indicates higher modal damping ratios.

3) The increase of R_m will increase the reaction of u_1 and u_2, so the mass of the additional layer should be minimized when designing the storey-adding steel structure. Moreover, when $0.6 < R_\omega < 1.2$, the effect of the damper on damping can be fully exerted so that a structural design with good seismic performance and economy can be achieved.

Acknowledgements

This study was supported in part by the National Natural Science Foundation of China through Grants 51078032, and by the Open Foundation of State Key Laboratory for Disaster Reduction in Civil Engineering (SLDRCE15-01). These support are gratefully acknowledged.

References

[1] Cheng X S, Jia C S, Zhang Y. Seismic Responses of an Added-Story Frame Structure with Viscous Dampers[J]. Mathematical Problems in Engineering, 2014, 2014: 1-9.
[2] Bahri F, Kafi M A, Kheyroddin A. Full-scale experimental assessment of new connection for columns in vertically mixed structures [J]. The Structural Design of Tall and Special Buildings, 2019, 28(12): 1-16.
[3] Lu X L, Zhu J J, Zou Y. Study on performance-based seismic design of Shanghai World Financial Center Tower[J]. Journal of Earthquake and Tsunami 2009;3(04): 273–284.
[4] Mehmet Alpaslan Köroğlu, Ali Köken, Yunus Dere. Use of different shaped steel slit dampers in beam to column connections of steel frames under cycling loading[J]. Advanced Steel Construction, 2018, 14(2): 251-273.
[5] Armouti N S. Effect of dampers on seismic demand of short period structures in Deep Cohesionless Sites [J]. Advanced Steel Construction, 2011, 7(2):192-205.
[6] Zhang Y X, Liu A R, Zhang A L, Liu X C. Seismic performance analysis of a resilient prestressed steel frame with intermediate column containing friction dampers[J]. Advanced Steel Construction, 2017, 13(3): 241-257.
[7] GB50011. Code for Seismic Design of Buildings in China; 2010 in Chinese.
[8] European committee for standardization. Eurocode 8 Design provisions for earthquake resistance of structures. ENV1998.
[9] Chen G, Soong T T. Exact solutions to a class of structure-equipment systems [J]. Journal of Engineering Mechanics, 1996;122(11):1093–100.
[10] Medina R A, Sankaranarayanan R, Kingston K M. Floor response spectra for light components mounted on regular moment-resisting frame structures [J]. Engineering Structures, 2006;28:1927–40.
[11] Papageorgiou A V, Gantes C J. Decoupling criteria for inelastic irregular primary/secondary structural systems subject to seismic excitation[J]. Journal of Engineering Mechanics, 2010, 136(10): 1234-1247.
[12] Cronin D L. Approximation for Determining Harmonically Excited Response of Non-classically Damped Systems [J]. Journal of Manufacturing Science & Engineering, 1976, 98(1): 43-47.
[13] Huang B C, Leung A Y T, Lam K L, Cheung V K. Analytical determination of equivalent modal damping ratios of a composite tower in wind-induced vibrations [J]. Computers & Structures, 1996; 59(2): 311–6.
[14] Papageorgiou A V, Gantes C J. Equivalent modal damping ratios for concrete/steel mixed structures [J]. Computers & Structures, 2010, 88(19-20): 1124-1136.
[15] Roesset J M, Whitman R V, Dobry R. Modal analysis for structures with foundation interaction[J]. ASCE Journal of the structural division 1973;99(3): 399–416.
[16] Zhang R F, Wang C, Pan C, Shen H, Ge Q Z, Zhang L Q. Simplified design of elastoplastic structures with metallic yielding dampers based on the concept of uniform damping ratio [J]. Engineering Structures, 2018, 176:734-745.
[17] Farghaly, Abdelraheem A. Parametric study on equivalent damping ratio of different composite structural building systems[J]. International Journal of Steel Structures, 2015, 15(1):7-16.
[18] Hwang Jae-Seung, Rha Chang-Soon. Equivalent Damping Ratio Identification of a Non-classically Damped Structure with Vibration Control System [J]. Journal of the Wind Engineering Institute of Korea, 2017, 21(3): 121-126.
[19] Sivandi-Pour A, Gerami M, Kheyroddin A. Uniform Damping Ratio For Non-Classically Damped Hybrid Steel Concrete Structures[J]. International Journal of Civil Engineering, 2016, 14(1):1-11.
[20] Huang W, Qian J, Zhou Z, Fu Q. An approach to equivalent damping ratio of vertically mixed structures based on response error minimization [J]. Soil Dynamics and Earthquake Engineering, 2015, 72: 119-128.
[21] Ashory M R, Ghasemi-Ghalebahman A, Kokabi M J. An efficient modal strain energy-based damage detection for laminated composite plates[J]. Advanced Composite Materials, 2017(2): 147-162.
[22] Alfouneh M, Tong L. Maximizing modal damping in layered structures via multi-objective topology optimization [J]. Engineering Structures, 2017, 132: 637-647.
[23] Noll S, Dreyer J, Singh R. Complex eigensolutions of coupled flexural and longitudinal modes in a beam with inclined elastic supports with non-proportional damping [J]. Journal of Sound and Vibration, 2014, 333(3):818-834.
[24] Bai B, Bai G C, Fei C W, Tong X. Application of Improved Hybrid Interface Substructural Component Modal Synthesis Method in Dynamic Characteristics Analysis of Mistuned Bladed Disk Assemblies [J]. Journal of Mechanical Engineering, 2015, 51(9): 73-81.
[25] Warburton G B, Soni S R. Errors in response calculations for non-classically damped structures [J]. Earthquake Engineering & Structural Dynamics, 1977, 5(4):365-376.
[26] Udwadia F E. A note on nonproportional damping [J]. Journal of Engineering Mechanics, 2009, 135(11): 1248-1256.
[27] Ibrahimbegovic A, Wilson E L. Simple numerical algorithms for the mode superposition analysis of linear structural systems with non-proportional damping[J]. Computers & Structures, 1989, 33(2): 523-531.
[28] Kim C W. A preconditioned iterative method for modal frequency-response analysis of structures with non-proportional damping[J]. Journal of Sound and Vibration, 2006, 297(3-5):1097-1103.
[29] Matteo Aureli. A framework for iterative analysis of non-classically damped dynamical systems[J]. Journal of Sound and Vibration, 2014, 333(24): 6688-6705.
[30] Foss K A. Coordinates which uncouple the equation of damped linear dynamic system [J]. Journal of Applied Mechanics-ASME, 1958, 25(1): 361-364.
[31] Cha P D. Approximate eigensolutions for arbitrarily damped nearly proportional systems [J]. Journal of Sound and Vibration, 2005, 288(4-5): 813-827.
[32] Hračov S, Náprstek J. Approximate complex eigensolution of proportionally damped linear systems supplemented with a passive damper [J]. Procedia Engineering, 2017, 199, 1677–1682.
[33] Pan D G, Fu X Q, Chen Q J, Lu P, Tan J P. A Modal Perturbation Method for eigenvalue Problem of Non-Proportionally Damped System [J]. Applied Science, 2020, 10(1), 341.
[34] Ragget J D. Estimating damping of real structure [J]. Journal of the Structural Division, 1975, 101(ST9): 1823-1835.
[35] D'Aveni A , Muscolino G . Response of non-classically damped structures in the modal subspace[J]. Earthquake Engineering & Structural Dynamics, 1995, 24(9):1267-1281.
[36] Veletsos A S, Ventura C E. Modal analysis of non-classically damped linear systems[J]. Earthquake Engineering & Structural Dynamics, 1986, 14, 217-243.
[37] Perotti, F. Analytical and numerical techniques for the dynamic analysis of non-classically damped linear systems [J]. Soil Dynamics and Earthquake Engineering, 1994, 13, 197–212.
[38] Tetsuji Itoh. Damped vibration mode superposition method for dynamic response analysis [J]. Earthquake Engineering and Structural Dynamics, 1973, 2, 47-57.
[39] Claret A M, Venancio-Filho F. A modal superposition pseudo-force method for dynamic analysis of structural systems with non-proportional damping [J]. Earthquake Engineering & Structural Dynamics, 1991, 20(4): 303-315.
[40] Pan D G, Chen G D, Lou M L. A modified modal perturbation method for vibration characteristics of non-prismatic Timoshenko beams[J]. Structural Engineering & Mechanics, 2011, 40(5):689-703.